catalysts

MDPI

Article

Surface Reduced CeO_2 Nanowires for Direct Conversion of CO_2 and Methanol to Dimethyl Carbonate: Catalytic Performance and Role of Oxygen Vacancy

Zhongwei Fu †, Yuehong Yu †, Zhen Li, Dongmei Han, Shuanjin Wang, Min Xiao * and Yuezhong Meng *

The Key Laboratory of Low-Carbon Chemistry & Energy Conservation of Guangdong Province/State Key Laboratory of Optoelectronic Materials and Technologies, Sun Yat-sen University, No. 135, Xingang Xi Road, Guangzhou 510275, China; fuzhw@mail2.sysu.edu.cn (Z.F.); yuyueh@mail2.sysu.edu.cn (Y.Y.); lizh63@mail2.sysu.edu.cn (Z.L.); handongm@mail.sysu.edu.cn (D.H.); wangshj@mail.sysu.edu.cn (S.W.)

* Correspondence: stsxm@mail.sysu.edu.cn (M.X.); mengyzh@mail.sysu.edu.cn (Y.M.); Tel.: +86-20-8411-4113 (Y.M.)

† These authors have contributed equally to this work.

Received: 14 March 2018; Accepted: 4 April 2018; Published: 19 April 2018

Abstract: Ultralong 1D CeO_2 nanowires were synthesized via an advanced solvothermal method, surface reduced under H_2 atmosphere, and first applied in direct synthesis of dimethyl carbonate (DMC) from CO_2 and CH_3OH. The micro morphologies, physical parameters of nanowires were fully investigated by transmission electron microscopy (TEM), X-ray diffraction (XRD), N_2 adsorption, X-ray photoelectron spectrum (XPS), and temperature-programmed desorption of ammonia/carbon dioxide (NH_3-TPD/CO_2-TPD). The effects of surface oxygen vacancy and acidic/alkaline sites on the catalytic activity was explored. After reduction, the acidic/alkaline sites of CeO_2 nanowires can be dramatically improved and evidently raised the catalytic performance. CeO_2 nanowires reduced at 500 °C (CeO_2_NW_500) exhibited notably superior activity with DMC yield of 16.85 mmol gcat^{-1}. Furthermore, kinetic insights of initial rate were carried out and the apparent activation energy barrier of CeO_2_NW_500 catalyst was found to be 41.9 kJ/mol, much tiny than that of CeO_2_NW catalyst (74.7 KJ/mol).

Keywords: dimethyl carbonate; carbon dioxide; ceria nanowires; oxygen vacancy

1. Introduction

As an environmentally benign compound and unique intermediate of versatile chemical products, dimethyl carbonate (DMC) is widely applied in polymer industry and pharmaceutical as well as detergent, surfactant, and softener additives [1,2]. In addition, DMC is important raw material when serving as a non-toxic substitute for poisonous phosgene and dimethyl sulfate in sustainable chemistry of carbonylation, methylation, and polymer synthesis [3,4]. As an additive, DMC can improve the octane number and oxygen content of fuels, thereby enhancing its antiknock [1]. Furthermore, DMC can be used as a cleaning solvent in coating paints and the important composition of electrolyte [5]. Considering the wide applications, DMC is known as the "new cornerstone" for synthesis chemistry nowadays and lots of efforts have been made in finding appropriate routes to meet the demand of DMC industrial production since it is far from satisfaction until now. Several approaches including the methanolysis of phosgene [6], the oxidative carbonylation of methanol [7], the transesterification of alkene carbonates [8], and the alcoholysis of urea [3], have been developed, but it is still limited with strict operation conditions, highly toxicity, and corrosivity up to now.

Using carbon dioxide (CO_2) in DMC synthesis is particularly attractive since CO_2 is known as a recyclable and naturally abundant raw materials for the production of plentiful chemical reagents. Meanwhile, the emissions of CO_2 have significantly increased and contributed to global warming, thus the utilization of CO_2 has attracted more and more attention in the last decades [9,10]. In this regard, the direct synthesis of DMC from CO_2, and methanol (Scheme 1) is considered as one of the most attractive and effective methods since such an approach is environmentally benign not only for reduction of greenhouse gas emissions but also for development of a new carbon resource [11,12]. However, such a sustainable route also exists significant challenges due to facts including the highly thermodynamically stability of CO_2, as well as the kinetically inert and deactivation of catalysts induced by water formation in the reaction process [13–15].

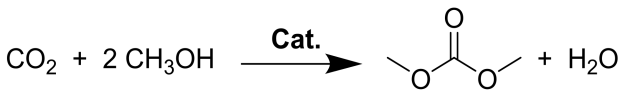

Scheme 1. Direct synthesis of DMC from CO_2 and methanol.

Several methods, such as adding co-reagents and dehydrants in the reaction systems, have been developed [16,17]. Furthermore, some new technologies, such as photo-assistant [14], electro-assistant [18], membrane separation [19], and supercritical CO_2 technology [20,21] have been introduced to boost the production of DMC in former reports. Even then, the reactions are preferred at strict conditions and the yield of DMC is relatively low. Though the efforts to these approaches are devoted today, the explorations of advanced heterogeneous catalysts are still regarded as the most effective route [22–24]. In particular, CeO_2 based catalysts have been transplanted in the direct synthesis of DMC and show much better catalytic activity as an excellent heterogeneous catalyst [25,26]. Plenty of references has employed CeO_2 as competent catalysts in DMC formation involving dehydration [27]. Furthermore, previously studies have revealed that the different crystal facets exposed on the surface of CeO_2 nanostructures were strongly controlled by its morphology, leading to differential physicochemical properties and further effecting the catalytic performance [28]. In this context, 1D structured CeO_2 nanorods catalyst demonstrated superior DMC yield (0.906 mmol DMC/mmol cat) from CO_2 and methanol when compared to CeO_2 nanocubes (0.582 mmol DMC/mmol cat) and CeO_2 nano-octahedrons (0.120 mmol DMC/mmol cat) [25,29]. However, major drawbacks of CeO_2 nanorods are the extremely low yield and high cost of hydrothermal method, preventing it from being used in practical applications [30]. In the meantime, the low aspect ratio of nanorods limits the specific surface area of catalysts, which would affect the catalytic performance further [25,26].

In this respect, we were especially interested in new trials for ultralong 1D CeO_2 nanostructure. Furthermore, oxygen deficiency of the CeO_2 based catalyst has been proved playing important roles in CO_2 and methanol activation in former research [26,31]. Thus, we conducted further research on surface reduced CeO_2 nanowires catalyst. Herein, CeO_2 nanowires with a diameter of 10 nm and an aspect ratio of more than 50 was successfully prepared by the refluxing approach established by Yu et al. [32] and then simply surface reduced under hydrogen atmospheres, followed by their application in the direct synthesis of DMC from CO_2 and methanol. Moreover, the influence of surface oxygen-deficiency and acid-basic sites were fully investigated. The catalytic recyclability was also detected. Finally, we conducted a detailed kinetic investigation for the direct formation of DMC in an autoclave reactor over catalysts.

2. Results and Discussion

2.1. Morphology and Microstructure of the Prepared Catalysts

CeO_2 nanowires catalyst was prepared using a solvothermal method in a mixed water/ethanol solvents (v/v = 1:1). Figure 1a,b show the morphology of the unreduced CeO_2 nanowires catalyst,

exhibiting an intact nanowire structure with an average length of around 500 nm and a uniform diameter of less than 10 nm. After reduced with H_2, the nanowire structure was kept undestroyed, and the size of nanowires has made almost no change (Figure 1c). The crystal structures of CeO_2 nanowires catalysts were investigated by XRD, and the spectra are shown in Figure 2. For unreduced CeO_2 nanowires, the diffraction peaks of 2θ can be ascribed to the fluorite-structured CeO_2 (JCPDS 34-0394, 28.6° (111), 33.1° (200), 47.6° (220), and 56.4° (311)). After reduction under H_2 atmosphere as a function of temperature (450–700 °C), the spectra of nanowires remained almost unchanged, indicating that the crystalline stucture of the nanowires was not destroyed.

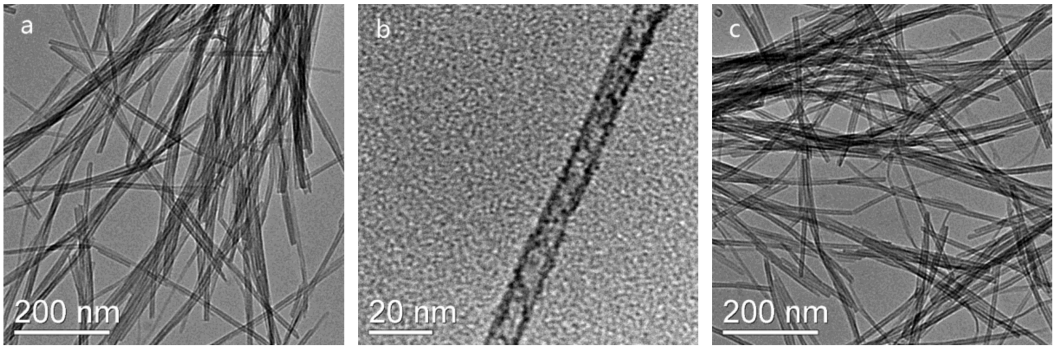

Figure 1. TEM images of (**a**,**b**) CeO_2_NW, and (**c**) CeO_2_NW_500.

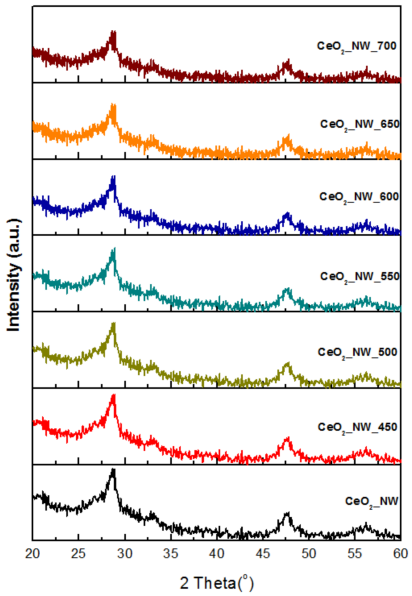

Figure 2. XRD patterns of CeO_2 nanowires reduced by H_2 as a function of temperature (450–700 °C).

Physical and chemical parameters of the as-prepared catalysts are summarized in Table 1. The specific surface area of the nanowires was acquired from BET method and seemed to decrease slightly from 116.33 m^2g^{-1} to 98.1 m^2g^{-1} upon increasing the reduction temperature up to 500 °C, indicating that the low-temperature reduction only can influence the specific surface area within tolerable extent. When elevating the reduction temperature, specific surface area of reduced CeO_2 nanowires drops abruptly, which inevitably lead to the covered up of efficient active sites and eventually cause the worse catalytic performance.

Further investigation on the surface acidic/alkaline properties of as-prepared catalysts was acquired by NH_3/CO_2-TPD. The amount of moderate acidic and alkaline sites is also summarized in Table 1. For CeO_2_NW_450 and CeO_2_NW_500, more plentiful moderately acidic and alkaline sites are

generated with the elevating of reduction temperature, which is bond to benefit the DMC formation according to former research. [33] While for other nanowires reduced under higher temperature, the amount of moderate acidity and alkalinity lessens. It can be ascribe to the fast-declining specific surface area upon elevating the reduction temperature, and then result in the covered up of efficient active sites. CeO_2_NW_500 was determined to possess both the richest acidity and alkalify, which is mainly because of the enriching of oxygen vacancy on catalysts surface, further providing much richer active sites when compared to unreduced nanowires.

Table 1. Textural data of as-prepared catalysts basing on BET, XRD, and XPS investigation.

Catalysts	BET Surface Area (m^2g^{-1})	Sites Amount ($\mu mol\ g^{-1}$)		Oxygen Vacancy (%)
		Moderate Acidity	Moderate Alkalify	
CeO_2_NW	116.3	82	25	5.1
CeO_2_NW_450	104.9	190	52	14.2
CeO_2_NW_500	98.1	282	82	20.5
CeO_2_NW_550	70.4	235	65	22.7
CeO_2_NW_600	55.2	192	48	25.1
CeO_2_NW_650	42.5	171	47	27.3
CeO_2_NW_700	28.7	115	39	31.2

Surface chemical state of prepared catalysts was investigated by XPS. Based on the calculated result, the XPS result forecasts that the oxygen vacancy on the surface of as-prepared nanowires varies along the reduction temperature from 5.1% in CeO_2_NW to 31.2% in CeO_2_NW_700. Due to the Ce valent state partly shift from +4 to +3, reduction of CeO_2 nanowires leads to the formation of oxygen vacancy on the catalyst surface.

Based on the aforesaid result, a certain relationship between the surface active sites (mainly the moderate acidic and alkaline sites), specific surface area and surface oxygen vacancy was established. Both the moderate acidic and alkaline sites showed a linear relationship contrast specific surface area multiply surface oxygen vacancy (Figure 3). The combination of TPD, XPS, and BET reveals that the oxygen vacant structure of nanowires contributes to the formation of moderately acidic and basic sites, which is also influenced by the specific surface area.

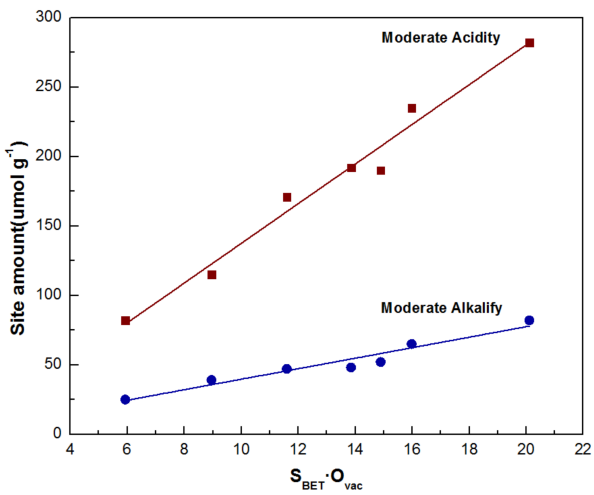

Figure 3. Liner relationship of moderate acidic/alkaline sites contrast specific surface area and surface oxygen vacancy.

2.2. Catalytic Performance

The effects of reduction temperature for nanowires on the catalytic activity were probed and the catalytic reaction was conducted in a stainless autoclave micro-reactor with high-speed stirring.

The DMC yield of as-prepared catalysts with different catalysts are demonstrated in Figure 4 and serves as the basis for original selection of reduction temperatures.

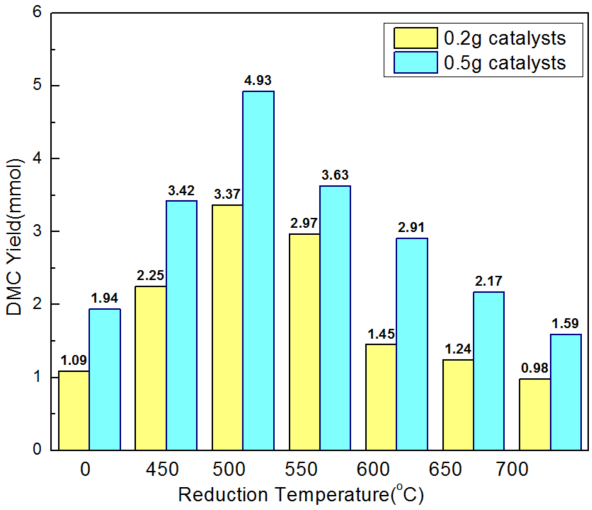

Figure 4. Effects of reduction temperature on the DMC yield over as-prepared nanowires. Reaction conditions: Methanol 500 mmol; catalysts 0.2 g or 0.5 g; CO_2 pressure 5 MPa; temperature 120 °C; reaction time 5 h.

Unreduced CeO_2 nanowires (CeO_2_NW) catalyst obtained much inferior DMC yield when compared with the surface reduced CeO_2 nanowires (CeO_2_NW_x). DMC yield enhanced with elevating the reduction temperature of CeO_2 nanowires, reached a maximum at 500 °C and then declined with further temperature rise. We observed the catalytic performance of all nanowires catalysts with loading amount of 0.2 g and 0.5 g respectively. The reaction found to reach saturated and catalytic performance was influenced by leveling effect when loading 0.5 g catalyst, while the catalyst was efficiently utilized at 0.2 g. Among the catalysts examined, CeO_2_NW_500 catalyst achieves excellent DMC yield of 16.85 mmol gcat^{-1}, superior than the catalytic activity of CeO_2_NW catalyst (5.45 mmol gcat^{-1}) under the same condition. Associating with the specific surface area of as-prepared catalysts, CeO_2_NW_x (x > 500) catalysts with tinier surface area proof inferior catalytic activity, illustrating that the catalytic performance is directly related to the specific surface area of as-prepared catalysts. Smaller specific surface area necessarily leads to the covering of efficient active sites and causes lower catalytic activity [34,35].

Further research on direct synthesis of DMC from $CO_2$and methanol over CeO_2_NW_500 was conducted. The effects of different catalytic conditions was fully investigated. Figure 5 shows the DMC amount with different reaction time and reaction temperatures over CeO_2_NW_500 catalysts catalyst. The generation rate of the destination product DMC enhanced when elevated the catalytic temperature, while the final yield of DMC constantly decreased due to the limitations of thermodynamic and generation of side product. Under 140 °C, the yield of DMC reached the maximum value at 75 min, and then seemed to be almost unchanged. However, the formation amount of DMC even trends increasing after 5 h at 120 °C.

Further investigation for the recyclability of CeO_2_NW_500 was carried out and the used nanowires catalyst was thermal reduced under H_2 atmosphere before re-catalyze the direct synthesis of DMC under the same reaction conditions. BET specific surface area and catalytic performance of the recovered CeO_2_NW_500 catalysts are demonstrated in Figure 6. Both specific surface area and the catalytic performance were found mildly falling as the number of reuses accumulates, which is on account of the slight surface collapse during the retreatment of the catalysts. Anyway, CeO_2_NW_500 shows favorable stability for the direct formation of DMC from CO_2 and methanol.

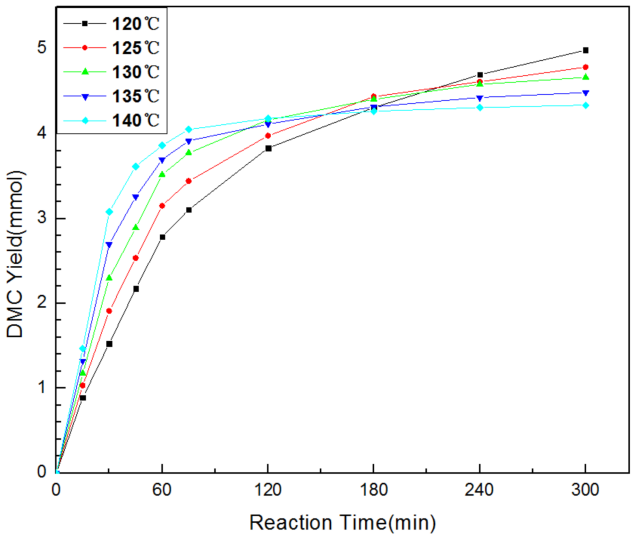

Figure 5. Effects of reaction temperature of nanowires on the catalytic performance for DMC formation. Reaction conditions: Methanol 500 mmol; CeO_2_NW_500 catalysts 0.5 g; CO_2 pressure 5 MPa.

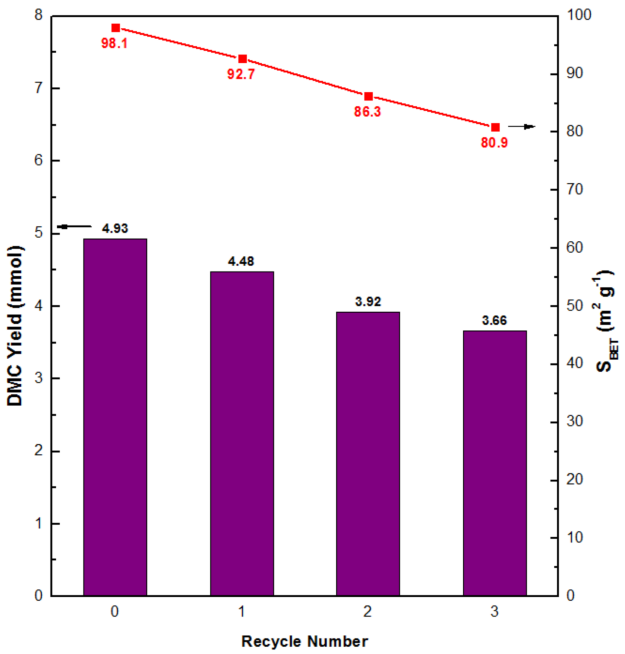

Figure 6. Recyclability study of CeO_2_NW_500 catalyst for the direct synthesis of DMC from CO_2 and methanol. Reaction conditions: Methanol 500 mmol; catalysts 0.5 g; CO_2 pressure 5 MPa; temperature 120 °C; reaction time 5 h.

2.3. Kinetic Analysis

Initial rate kinetic insights in the direct synthesis of DMC over CeO_2_NW_500 catalyst were conducted. Based on the result of Figure 5, the yield data within 60 min was selected as the initial rate region. In addition, similar initial reaction was carried out on CeO_2_NW and compared with that of CeO_2_NW_500. The linear fitting of Arrhenius plot in Figure 7 gives a slope at −5.04 (±0.41), indicating the apparent activation energy at 41.9 ± 3.4 kJ/mol for CeO_2_NW_500 catalyst, which is lower than CeO_2_NW catalyst (74.7 kJ/mol). It suggests that the surface reduction of CeO_2 nanowires has reduced the activation energy barriers and improved the catalytic performance by enriching the surface active sites.

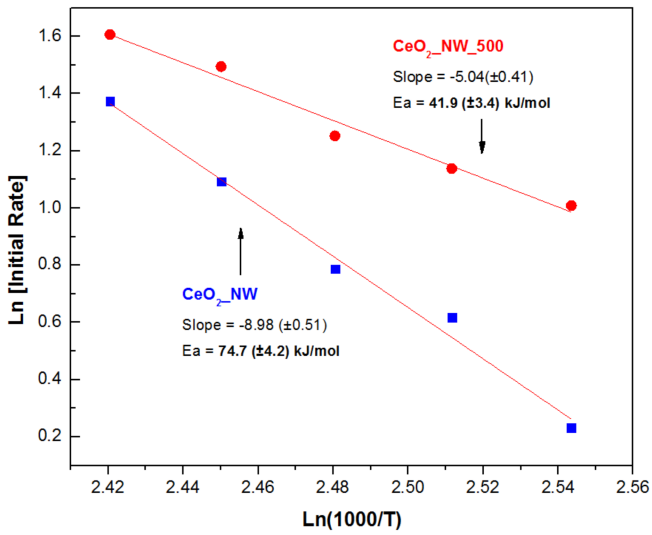

Figure 7. Arrhenius plot for direct synthesis of DMC over CeO_2_NW_500 and CeO_2_NW catalyst.

Furthermore, based on the former proposed mechanism for the direct synthesis of DMC, surface adsorption and activation of CO_2 and methanol occurs on the alkaline sites and acidic sites, respectively [36]. As a consequence, the inferior catalytic performance of unreduced CeO_2_NW catalyst in this study should mainly ascribe to much poorer surface acidic and alkaline sites. While for CeO_2_NW_x catalysts, more abundant moderately acidic and alkaline sites generate along with the surface reduction process, thus resulting in more favorable catalytic performance than CeO_2_NW. Figure 8 shows the Ln–Ln curves of initial rate for each catalysts contrast the concentration of moderately acidic/alkaline sites. There is a positive liner relationship of these parameters, suggesting the initial rates of this reaction influenced by the activation of both CO_2 and methanol. This result corresponds to the deduction of Langmuir–Hinshelwood mechanism [37,38].

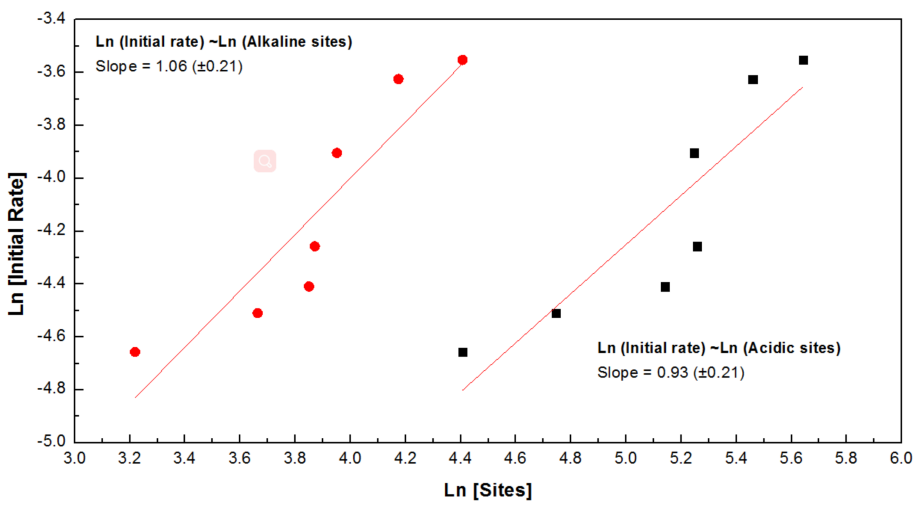

Figure 8. Kinetics study of the initial rate of DMC production contrast acidic/alkaline sites. Reaction conditions: Methanol 500 mmol; catalysts 0.2 g; CO_2 pressure 5 MPa; temperature 120 °C; reaction time 60 min.

3. Materials and Methods

3.1. Materials

Cerium (III) nitrate hexahydrate $Ce(NO_3)_3 \cdot 6H_2O$, methanol, and dimethyl carbonate (DMC) were purchased from Aladdin Co., Ltd. (Shanghai, China). Ammonium hydroxide $NH_3 \cdot H_2O$ (25 wt %) and ethanol was purchased from Guangdong Chemical Reagent Factory (Guangzhou, China). All the reactants were of analytical purity and used without any further treatment.

High purity CO_2 (>99.9999%) and H_2 (>99.999%) were obtained from Guangqi Gas Co., Ltd. (Guangzhou, China).

3.2. Catalysts Preparation

Ceria nanowires catalyst was prepared using a solvothermal method in a mixed water/ethanol solvents [32]. Briefly, stoichiometric $Ce(NO_3)_3 \cdot 6H_2O$ was dissolved in a flash with water/ethanol mixed solution (v/v = 1:1), following by oil bath heating up to 140 °C. Then the $NH_3 \cdot H_2O$ was added into the flash and the reaction mixture was refluxed for 12 h under stirring. After cooling to room temperature, the resulting mixture was separated by centrifugation. Afterward, the solid product was bathed with a mixture of ethanol and water (v/v = 1:1) for several times. After that, the pre-synthesized nanowires were freeze-dried in a lyophilizer (Four-Ring Science Instrument Plant Beijing Corporation, Beijing, China) at a vacuity of 3 mbar and a frigorific temperature of −40 °C. Finally, as-prepared nanowires catalyst were thermal reduced under H_2 atmosphere for 4 h. The samples were named after CeO_2_NW and CeO_2_NW_x, in which x represented the reduced temperature.

3.3. Catalyst Characterization

Micromorphology measurement was carried out on a transmission electron microscope (TEM, JSM-2010HR, JEOL Ltd., Tokyo, Japan) at a high voltage of 200 kV. Samples were ultrasonic dispersed into ethanol absolute, and then dropwise loaded onto the micro copper grid, followed by drying under air condition at room temperature.

Powder X-ray diffraction (XRD) was measured on a XRD diffractometer (Dmax 2200, Rigaku Ltd., Tokyo, Japan) at a scan rate of 5°/min. High voltage of 40 kV and current of 30 mA were employed in this measurement and Cu Kα radiation target (λ = 0.154178 nm) was used.

N_2 adsorption characterization was acquired on a nitrogen adsorption apparatus (ASAP-2020, Micrometrics Ltd., Cumming, GA, USA) and the specific surface area was calculated through the Brunauer–Emmett–Teller method from the adsorption results. Samples were pre-treated under nitrogen atmosphere at 200 °C for 2 h. After cooling, N_2 at a flow rate of 110 mL/min was adsorbed on the samples surface in a U tube surrounded by liquid nitrogen.

Temperature programmed desorption (TPD) was conducted on a chemical adsorption apparatus (Chem-BET 3000, Quantachrome Ltd., Boynton Beach, FL, USA). Firstly, samples were pre-treated under nitrogen atmosphere at 200 °C for 1 h. Then, a mixture standard gas of 10%CO_2/90%N_2 or 10%NH_3/90%N_2 saturated with the samples for 30 min at a flow rate of 60 mL/min in a U tube. After that, surface physical adsorption of CO_2 or NH_3 was dislodged by bathing with 30%N_2/70% He standard gas for 2 h at a flow rate of 50 mL/min. Then, the samples were thermal treated under N_2/He 30%N_2/70% He from room temperature up to 600 °C with 8 °C/min heating rate. Finally, the total desorption of NH_3/CO_2 was determined through back-titration method. HCl/NaOH (0.01 mol/L) was employed as an adsorbent for NH_3/CO_2, NaOH/HCl (0.01 mol/L) was served as titrant together with a mixed indicator reagent, which consisted of bromocresol green ethanol solution (1%, 3 equivalent volumes) and methyl red ethanol solution (2%, 1 equivalent volume) [39].

X-ray photoelectron spectrum (XPS) was acquired on an X-ray photoelectron spectrometer (ESCALAB250, Thermo Fisher Scientific Ltd., Waltham, MA, USA) with a scan survey of 1100-0 eV binding energy range. Monochromatized Al-Ka source at 1486.6 eV and 150 w was applied in the

characterization with a voltage of 15 kV. Surface oxygen vacancy can be roughly calculated according to the equation

$$O_{Vac}\ (\%)\ = \frac{C(Ce)\ - 0.5\ C(O)}{C(Ce)} \quad (1)$$

3.4. Catalytic Performance Measurement

Direct synthesis of DMC from CO_2 and methanol was carried out in a stainless steel autoclave with a volume of 50 mL and high-velocity stirring. As-prepared catalyst and a certain amount of absolute methanol were added into the reactor, following be purging CO_2 for several times to evacuate the air inside and obtained the strict oxygen-free and water-free condition. Reaction pressure of CO_2 was set at 5 MPa and the reaction was conducted at 120 °C for 5 h if no otherwise specified. The final products were measured and quantified by a gas chromatograph (GC-7900II, Techcomp Ltd., Beijing, China) equipped with a flame ionization detector (FID) after filtrating with PES membrane with a pore size of 0.45 um.

4. Conclusions

Ultralong 1D CeO_2 nanowires were synthesized via an advanced solvothermal method, surface reduced under H_2 atmosphere, and firstly applied in direct synthesis of dimethyl carbonate (DMC) from CO_2 and CH_3OH. The influences of reduction temperatures for the nanowires and different operating conditions for the catalysis reactivity were fully explored. The catalysis reactivity of ceria nanowires was founded to be greatly improved after surface reduction by generating more surface acidic-alkaline sites. Among the catalysts investigated, CeO_2_NW_500 obtains the most favorable catalytic activity for DMC formation than CeO_2_NW and all of the other CeO_2_NW_x catalysts. Under optimal reaction conditions, CeO_2_NW_500 catalyst achieves the best catalysis reactivity with DMC yield of 16.85 mmol gcat^{-1} in an autoclave reactor. Based on the approach of initial rates method, the kinetic insight were conducted for the direct synthesis of DMC over CeO_2_NW_500 catalyst and the activation energy barrier is determined to be 41.9 kJ/mol, tinier than 74.7 kJ/mol for unreduced CeO_2 nanowires. Moreover, a certain relationship between the initial rate and the surface acidity/alkalify was found, which is identical to the deduction of former proposed Langmuir–Hinshelwood mechanism where the initial rates of this reaction are influenced by the activation of both CO_2 and methanol.

Acknowledgments: The authors would like to thank the National Natural Science Foundation of China (grant no. 21376276, 21643002), Guangdong Province Sci. & Tech. Bureau (grant no. 2017B090901003, 2016B010114004, 2016A050503001), and Fundamental Research Funds for the Central Universities (171gjc37) for financial support of this work.

Author Contributions: Zhongwei Fu, Yuezhong Meng, Min Xiao, Dongmei Han, and Shuanjin Wang conceived and designed the experiments; Zhongwei Fu performed the experiments; Zhongwei Fu and Yuehong Yu analyzed the data; Zhen Li and Yuehong Yu contributed analysis tools; Zhongwei Fu wrote the paper.

Conflicts of Interest: The authors declare no conflict of interest.

References

1. And, M.A.P.; Christopher, L.M. Review of dimethyl carbonate (DMC) manufacture and its characteristics as a fuel additive. *Energy Fuels* **1997**, *11*, 2–29.
2. Ono, Y. Catalysis in the production and reactions of dimethyl carbonate, an environmentally benign building block. *Appl. Catal. A Gen.* **1997**, *155*, 133–166. [CrossRef]
3. Santos, B.A.V.; Silva, V.M.T.M.; Loureiro, J.M.; Rodrigues, A.E. Review for the direct synthesis of dimethyl carbonate. *Chem. Rev.* **2015**, *1*, 214–229. [CrossRef]
4. Keller, N.; Rebmann, G.; Keller, V. Catalysts, mechanisms and industrial processes for the dimethylcarbonate synthesis. *J. Mol. Catal. A Chem.* **2010**, *317*, 1–18. [CrossRef]
5. Tundo, P.; Selva, M. The chemistry of dimethyl carbonate. *Acc. Chem. Res.* **2002**, *35*, 706. [CrossRef] [PubMed]

6. Chaturvedi, D.; Mishra, N.; Mishra, V. Various approaches for the synthesis of organic carbamates. *Curr. Org. Synth.* **2007**, *4*, 308–320. [CrossRef]
7. King, S.T. Reaction mechanism of oxidative carbonylation of methanol to dimethyl carbonate in cu–y zeolite. *J. Catal.* **1996**, *161*, 530–538. [CrossRef]
8. Bhanage, B.M.; Fujita, S.; Ikushima, Y.; Torii, K.; Arai, M. Synthesis of dimethyl carbonate and glycols from carbon dioxide, epoxides and methanol using heterogeneous mg containing smectite catalysts: Effect of reaction variables on activity and selectivity performance. *Green Chem.* **2003**, *5*, 71–75. [CrossRef]
9. Zhao, G.; Huang, X.; Wang, X.; Wang, X. Progress in catalyst exploration for heterogeneous CO_2 reduction and utilization: A critical review. *J. Mater. Chem. A* **2017**, *41*, 21625–21649. [CrossRef]
10. Olajire, A.A. Recent advances in the synthesis of covalent organic frameworks for CO_2 capture. *J. CO_2 Util.* **2017**, *17*, 137–161. [CrossRef]
11. Fu, Z.; Meng, Y. *Research Progress in the Phosgene-Free and Direct Synthesis of Dimethyl Carbonate From CO_2 and Methanol*; Springer International Publishing: Berlin/Heidelberg, Germany, 2016.
12. Garciaherrero, I.; Cuéllarfranca, R.M.; Alvarezguerra, M.; Irabien, A.; Azapagic, A. Environmental assessment of dimethyl carbonate production: Comparison of a novel electrosynthesis route utilizing CO_2 with a commercial oxidative carbonylation process. *ACS Sustain. Chem. Eng.* **2016**, *4*, 2088–2097. [CrossRef]
13. Fang, S.; Fujimoto, K. Direct synthesis of dimethyl carbonate from carbon dioxide and methanol catalyzed by base. *Appl. Catal. A Gen.* **1996**, *142*, L1–L3. [CrossRef]
14. Wang, X.J.; Xiao, M.; Wang, S.J.; Lu, Y.X.; Meng, Y.Z. Direct synthesis of dimethyl carbonate from carbon dioxide and methanol using supported copper (Ni, V, O) catalyst with photo-assistance. *J. Mol. Catal. A Chem.* **2007**, *278*, 92–96. [CrossRef]
15. Han, D.; Wang, S.; Meng, Y.; Chen, Y.; Lu, Y.; Xiao, M. Porous diatomite-immobilized cu–ni bimetallic nanocatalysts for direct synthesis of dimethyl carbonate. *J. Nanomater.* **2012**, *2012*, 8.
16. Eta, V.; Mäkiarvela, P.; Murzin, D.Y.; Salmi, T.; Mikkola, J.P. Synthesis of dimethyl carbonate from methanol and carbon dioxide : The effect of dehydration. *Ind. Eng. Chem. Res.* **2009**, *49*, 9609–9617. [CrossRef]
17. Lin, C.M.; Shen, D.P.; You, Y.U.; Ming-Xian, X.U. Catalysts and dehydration agents of one-pot synthesis of dimethyl carbonate. *J. Zhejiang Univ. Technol.* **2013**, *13*, 329–331.
18. Zhou, Y.; Fu, Z.; Wang, S.; Xiao, M.; Han, D.; Meng, Y. Electrochemical synthesis of dimethyl carbonate from CO_2 and methanol over carbonaceous material supported dbu in a capacitor-like cell reactor. *RSC Adv.* **2016**, *6*, 40010–40016. [CrossRef]
19. Mengers, H.J. Membrane reactors for the direct conversion of CO_2 to dimethyl carbonate. *Clin. Nephrol.* **2015**, *33*, 1653–1659.
20. Ballivet-Tkatchenko, D.; Ligabue, R.A.; Plasseraud, L. Synthesis of dimethyl carbonate in supercritical carbon dioxide. *Braz. J. Chem. Eng.* **2006**, *23*, 111–116. [CrossRef]
21. Hong, S.T.; Park, H.S.; Lim, J.S.; Lee, Y.W.; Anpo, M.; Kim, J.D. Synthesis of dimethyl carbonate from methanol and supercritical carbon dioxide. *Res. Chem. Intermed.* **2006**, *32*, 737–747. [CrossRef]
22. Bian, J.; Xiao, M.; Wang, S.; Lu, Y.; Meng, Y. Direct synthesis of dmc from CH_3 oh and CO_2 over v -doped cu–ni/ac catalysts. *Catal. Commun.* **2009**, *10*, 1142–1145. [CrossRef]
23. Chen, H.; Wang, S.; Xiao, M.; Han, D.; Yixin, L.U.; Meng, Y. Direct synthesis of dimethyl carbonate from coand choh using 0.4 nm molecular sieve supported cu-ni bimetal catalyst. *Chin. J. Chem. Eng.* **2012**, *20*, 906–913. [CrossRef]
24. Zhang, M.; Xiao, M.; Wang, S.; Han, D.; Lu, Y.; Meng, Y. Cerium oxide-based catalysts made by template-precipitation for the dimethyl carbonate synthesis from carbon dioxide and methanol. *J. Clean. Prod.* **2015**, *103*, 847–853. [CrossRef]
25. Wang, S.; Zhao, L.; Wang, W.; Zhao, Y.; Zhang, G.; Ma, X.; Gong, J. Morphology control of ceria nanocrystals for catalytic conversion of CO_2 with methanol. *Nanoscale* **2013**, *5*, 5582–5588. [CrossRef] [PubMed]
26. Fu, Z.; Zhong, Y.; Yu, Y.; Long, L.; Xiao, M.; Han, D.; Wang, S.; Meng, Y. TiO_2-doped CeO_2 nanorod catalyst for direct conversion of CO_2 and CH_3OH to dimethyl carbonate: Catalytic performance and kinetic study. *ACS Omega* **2018**, *3*, 198–207. [CrossRef]
27. Honda, M.; Sonehara, S.; Yasuda, H.; Nakagawa, Y.; Tomishige, K. Heterogeneous CeO_2 catalyst for the one-pot synthesis of organic carbamates from amines, CO_2 and alcohols. *Green Chem.* **2011**, *13*, 3406–3413. [CrossRef]

28. Sun, C.; Li, H.; Zhang, H.; Wang, Z.; Chen, L. Controlled synthesis of ceo2 nanorods by a solvothermal method. *Nanotechnology* **2005**, *16*, 1454. [CrossRef]
29. Zhao, S.Y.; Wang, S.P.; Zhao, Y.J.; Ma, X.B. An in situ infrared study of dimethyl carbonate synthesis from carbon dioxide and methanol over well-shaped CeO_2. *Chin. Chem. Lett.* **2017**, *28*, 65–69. [CrossRef]
30. Vantomme, A.; Yuan, Z.Y.; Du, G.; Su, B.L. Surfactant-assisted large-scale preparation of crystalline CeO_2 nanorods. *Langmuir ACS J. Surf. Colloids* **2005**, *21*, 1132. [CrossRef] [PubMed]
31. Watanabe, S.; Ma, X.; Song, C. Characterization of structural and surface properties of nanocrystalline TiO_2-CeO_2 mixed oxides by XRD, XPS, TPR, and TPD. *J. Phys. Chem.C* **2009**, *113*, 14249–14257. [CrossRef]
32. Yu, X.F.; Liu, J.W.; Cong, H.P.; Xue, L.; Arshad, M.N.; Albar, H.A.; Sobahi, T.R.; Gao, Q.; Yu, S.H. Template- and surfactant-free synthesis of ultrathin CeO_2 nanowires in a mixed solvent and their superior adsorption capability for water treatment. *Chem. Sci.* **2015**, *6*, 2511. [CrossRef] [PubMed]
33. Li, A.; Pu, Y.; Li, F.; Luo, J.; Zhao, N.; Xiao, F. Synthesis of dimethyl carbonate from methanol and CO_2 over fe–zr mixed oxides. *J. CO_2 Util.* **2017**, *19*, 33–39. [CrossRef]
34. Li, H.; Jiao, X.; Li, L.; Zhao, N.; Xiao, F.; Wei, W.; Sun, Y.; Zhang, B. Synthesis of glycerol carbonate by direct carbonylation of glycerol with CO_2 over solid catalysts derived from zn/al/la and zn/al/la/m (m = li, mg and zr) hydrotalcites. *Catal. Sci. Technol.* **2015**, *5*, 989–1005. [CrossRef]
35. Cosimo, J.I.D.; DıEz, V.K.; Xu, M.; Iglesia, E.; ApesteguıA, C.R. Structure and surface and catalytic properties of mg-al basic oxides. *J. Catal.* **1998**, *178*, 499–510. [CrossRef]
36. Jung, K.T.; Bell, A.T. An in situ infrared study of dimethyl carbonate synthesis from carbon dioxide and methanol over zirconia. *J. Catal.* **2001**, *204*, 339–347. [CrossRef]
37. Tomishige, K.; Ikeda, Y.; Sakaihori, T.; Fujimoto, K. Catalytic properties and structure of zirconia catalysts for direct synthesis of dimethyl carbonate from methanol and carbon dioxide. *J. Catal.* **2000**, *192*, 355–362. [CrossRef]
38. Marin, C.M.; Li, L.; Bhalkikar, A.; Doyle, J.E.; Zeng, X.C.; Cheung, C.L. Kinetic and mechanistic investigations of the direct synthesis of dimethyl carbonate from carbon dioxide over ceria nanorod catalysts. *J. Catal.* **2016**, *340*, 295–301. [CrossRef]
39. Jin, D.; Jing, G.; Hou, Z.; Yan, G.; Lu, X.; Zhu, Y.; Zheng, X. Microwave assisted in situ synthesis of usy-encapsulated heteropoly acid (hpw-usy) catalysts. *Appl. Catal. A Gen.* **2009**, *352*, 259–264. [CrossRef]

© 2018 by the authors. Licensee MDPI, Basel, Switzerland. This article is an open access article distributed under the terms and conditions of the Creative Commons Attribution (CC BY) license (http://creativecommons.org/licenses/by/4.0/).